TOXICOLOGICAL SCIENCES, 162(1), 2018, 146–166

doi: 10.1093/toxsci/kfx235
Advance Access Publication Date: November 2, 2017
Research Article

Investigating the Generalizability of the MultiFlow ® DNA Damage Assay and Several Companion Machine Learning Models With a Set of 103 Diverse Test Chemicals

Steven M. Bryce,*,[1] Derek T. Bernacki,*,[1] Stephanie L. Smith-Roe,† Kristine L. Witt,† Jeffrey C. Bemis,* and Stephen D. Dertinger*,[2]

*Litron Laboratories, Rochester, New York; and †Division of the National Toxicology Program, National Institute of Environmental Health Sciences, Research Triangle Park, North Carolina.

1These authors contributed equally to this study.
[2]To whom correspondence should be addressed. E-mail: sdertinger@litronlabs.com.

ABSTRACT

The *in vitro* MultiFlow DNA Damage assay multiplexes p53, γH2AX, phospho-histone H3, and polyploidization biomarkers into 1 flow cytometric analysis (Bryce, S. M., Bernacki, D. T., Bemis, J. C., and Dertinger, S. D. (2016). Genotoxic mode of action predictions from a multiplexed flow cytometric assay and a machine learning approach. *Environ. Mol. Mutagen.* 57, 171–189). The work reported herein evaluated the generalizability of the method, as well as several data analytics strategies, to a range of chemical classes not studied previously. TK6 cells were exposed to each of 103 diverse chemicals, 86 of which were supplied by the National Toxicology Program (NTP) and selected based upon responses in genetic damage assays conducted under the Tox21 program. Exposures occurred for 24 h over a range of concentrations, and cell aliquots were removed at 4 and 24 h for analysis. Multiplexed response data were evaluated using 3 machine learning models designed to predict genotoxic mode of action based on data from a training set of 85 previously studied chemicals. Of 54 chemicals with sufficient information to make an *a priori* call on genotoxic potential, the prediction models' accuracies were 79.6% (random forest), 88.9% (logistic regression), and 90.7% (artificial neural network). A majority vote ensemble of the 3 models provided 92.6% accuracy. Forty-nine NTP chemicals were not adequately tested (maximum concentration did not approach assay's cytotoxicity limit) and/or had insufficient conventional genotoxicity data to allow their genotoxic potential to be defined. For these chemicals MultiFlow data will be useful in future research and hypothesis testing. Collectively, the results suggest the MultiFlow assay and associated data analysis strategies are broadly generalizable, demonstrating high predictability when applied to new chemicals and classes of compounds.

Key words: genotoxicity; mode of action; flow cytometry; machine learning; Tox21.

Evaluation of a chemical's genotoxic potential has traditionally involved multiple assays covering the disparate types of DNA damage, especially those resulting in gene mutation and chromosomal effects that include both structural and numerical changes (Cimino, 2006; Dearfield *et al.*, 1991). The use of several assays has arguably served public health well, as the typical batteries that have been employed over the years exhibit high sensitivity for detecting genotoxicants (Kirkland *et al.*, 2005). However, there are several recognized deficiencies with the conventional assays. First, most individual assays do not provide sufficient information about genotoxic mode of action (MoA). Second, conventional assays are resource intensive, and most of the endpoints that are measured are not compatible with high-throughput approaches, thus hindering increased

coverage of chemical space. Finally, batteries of assays require large amounts of test chemical, and the combination of results among several assays leads to low specificity (Kirkland *et al.*, 2005).

Isolated progress has been made in addressing some of these deficiencies. For example, in regard to low specificity, some reports suggest that use of p53-competent human cell lines rather than p53-deficient rodent cell lines may increase the relevance of the findings (Fowler *et al.*, 2012). In addition, the decision to reduce the limit concentration for *in vitro* testing of human pharmaceuticals to a more physiologically relevant level has recognized advantages (Galloway, 2017). In terms of MoA, several approaches have shown merit. Whereas CREST antibodies and FISH probes that help delineate genotoxic MoA are well established (Doherty *et al.*, 1996; Lynch and Parry, 1993), newer, higher throughput approaches have also been described. These include panels of engineered cell lines with fluorescent reporter output (Hendriks *et al.*, 2012; Nagel *et al.*, 2014), and utilization of nontraditional biomarkers sensitive to specific mode(s) of action (Audebert *et al.*, 2010; Cheung *et al.*, 2015; Garcia-Canton *et al.*, 2013; Muehlbauer and Schuler, 2005; Muehlbauer *et al.*, 2008; Nikolova *et al.*, 2014; Smart *et al.*, 2011).

In addition to the advances noted earlier, considerable work has been directed at reducing resource requirements and improving throughput capacity, eg, *via* evaluation of toxicogenomics signatures (Li *et al.*, 2015; Yauk *et al.*, 2016), automated scoring of *in vitro* micronuclei (Avlasevich *et al.*, 2006; Diaz *et al.*, 2007) and reconfiguration of the single cell gel electrophoresis (comet) assay for highly parallel processing (Ge *et al.*, 2015). Furthermore, in recognition that only a very small percentage of the approximately 80 000 chemicals used in commerce have undergone adequate toxicity testing, the NTP, as a partner in the Toxicity Testing in the 21st Century Initiative (Tox21), has used *in vitro*, quantitative high-throughput screening (qHTS) to rapidly gain toxicity data for a library of approximately 10 000 compounds (Tice *et al.*, 2013). Five of the approximately 40 Tox21 assays were included in the testing battery to detect potential genotoxicants. These assays detected changes in well-recognized biomarkers for DNA damage, such as p53 (Witt *et al.*, 2017) and γH2AX, but also lesser-known DNA damage markers, such as post-translational modification of ATAD5 (Fox *et al.*, 2012). Differential cytotoxicity between chicken lymphoblastoid DT40 cell lines deficient for distinct DNA repair pathways versus the isogenic wildtype DNA repair competent cell line has also been used to identify potential genotoxicants (Nishihara *et al.*, 2016; Yamamoto *et al.*, 2011).

An area of study pursued by our laboratories is the development of a multiplexed flow cytometric assay that combines information from several biomarkers relevant to DNA damage response pathways (Bernaki *et al.*, 2016; Bryce *et al.*, 2014, 2016, 2017). This method, commercially known as the MultiFlow DNA Damage assay, involves a 1-step, add-and-read process that prepares cells in microtiter plates for flow cytometric analysis. The biomarkers measured in the assay include phosphorylation of histone H3 (p-H3) and phosphorylation of H2AX at serine 139 (γH2AX) to identify mitotic cells and DNA double strand break repair foci, respectively; nuclear p53 content as an indicator of p53 translocation in response to DNA damage; frequency of 8n cells to monitor polyploidization; and determination of nuclei counts to provide information about treatment-related cytotoxicity. Earlier work described a data analysis strategy that used multinomial logistic regression (LR) to generate probability scores that classified chemicals according to their predominant MoA: clastogen, aneugen, or nongenotoxicant (Bryce *et al.*, 2016). More recently the assay was found to exhibit good transferability among 7 laboratories that studied 60 chemicals at 2 or more sites (Bryce *et al.*, 2017).

This study extends our work with the MultiFlow platform by evaluating the degree to which the biomarker response profiles observed to date could be generalized to new chemicals with known genotoxic activities. Additionally, we evaluated the extent to which the multinomial LR algorithms or other machine learning approaches could be applied to MultiFlow data generated from TK6 cells exposed to new chemicals (ie, compounds that were not used for model training or cross-validation purposes). The results of these investigations are presented herein, along with discussion about potential placements for scalable, multiplexed genotoxicity assays.

MATERIALS AND METHODS

Chemicals. The identity of 103 test chemicals, along with CAS Registry Number, source, and other information, is provided in Table 1. The National Toxicology Program's (NTP) chemical repository supplied 86 of the 103 as dimethyl sulfoxide (DMSO) solubilized chemicals (coded) to Litron, and these were stored frozen until use (−20 °C). These NTP chemicals, generally provided as 20 mM stock solutions, were selected to reflect a diversity of chemical classes and structures, as well as responses in 5 HTS assays for DNA damage and repair, and conventional genotoxicity assays. The identity and purity of each NTP-sourced chemical was confirmed through independent analysis (data not shown). Seventeen additional chemicals were selected by Litron in order to increase the number of presumed nongenotoxicants studied, and to include aneugenic agents, a class that was not well represented in the NTP chemical set. Our *a priori* expectation regarding the *in vitro* mammalian cell genotoxicity potential for each of the 103 chemicals can be found in Table 1. Two characteristics of these chemical sets and our *a priori* classifications are noteworthy. First, the emphasis of this work was to study chemicals for their ability to cause DNA damage directly, ie, without metabolic activation. Thus, when available conventional genotoxicity assay results suggested that a chemical is positive only upon metabolic activation, it was deemed an expected negative. Second, agents from the NTP chemical repository were limited in terms of the top concentration supplied. This explains why the NTP chemicals could not be tested to 1 mM as has been our routine practice (Bernacki *et al.*, 2016; Bryce *et al.*, 2016, 2017). Rather, the highest concentrations tested were approximately 200 μM, a level that could not be increased while still maintaining an acceptable final solvent concentration (ie, DMSO at 1% v/v).

As shown in Table 1, the chemicals were assigned 1 of 3 categories at the completion of testing in the MultiFlow assay. The "A" designation denotes chemicals that were deemed to be adequately tested, based on meeting one or both of the following criteria: tested to 1 mM concentration, and/or approached the assay's cytotoxicity limit (ie, 24 h relative nuclei count [RNC] between 40 and 20%). The "S" designation denotes chemicals that were tested up to their solubility limit. In these cases, precipitate was noted in the culture medium either shortly after addition of test article or at the 4 or 24 h sampling times. For these chemicals the lowest precipitating concentration was the highest concentration tested. The "I" category was reserved for chemicals that were inadequately tested. These agents did not exhibit significant evidence of genotoxicity in the MultiFlow assay under the present test conditions, but no call could be made because the chemicals were not tested to either 1 mM or a

Table 1. Test Chemical Information

Chemical	CAS No.	Source	**Test Group**[a]	Top Conc. (μM)	Other Genetox[b]	Mammalian Cell Genetox Expectation[c] (-S9)	References and Miscellaneous Notes
1-Decyl-3-methylimidazolium bis(trifluoromethylsulfonyl)imide	433337-23-6	IoLiTec Ionic Liquids Technologies Inc. *via* NTP	A	8.93	No NTP data, no publications	Insufficient data	NA
1-Methyl-3-tetradecylimidazolium bis(trifluoromethylsulfonyl)imide	404001-49-6	IoLiTec Ionic Liquids Technologies Inc. *via* NTP	A	4	No NTP data, no publications	Insufficient data	NA
1, 1, 3-Trichloropropanone	921-03-9	TCI America *via* NTP	A	6.31	Ames pos. (± S9), *in vitro* CA pos. (± S9, stronger without S9), *in vivo* mouse MN neg., *in vivo* MN pos. (newt larvae), not tested by NTP	Positive	Leadscope (http://www.leadscope.com), Blazak et al. (1988), and Le Curieux et al. (1994)
1, 2-Benzenediamine, N-phenyl-(a.k.a. N-Phenyl-o-phenylenediamine)	534-85-0	Sigma-Aldrich	A	50.25	No NTP data, no publications	Insufficient data	NA
1, 2-Phenylenediamine HCl2	615-28-1	Acros Organics *via* NTP	A	102	Ames pos., *in vitro* MLA, CA pos., *in vivo* MN pos.	Positive	EURL ECVAM Genotoxicity and Carcinogenicity Consolidated Database of Ames Positive Chemicals
2-Methoxy-3, 4-dihydro-2H-pyran	5/1/54	Acros Organics	A	25	*in vitro Hprt* pos. (-S9)	Positive	BG RCI Toxicological Evaluations, no. 266
2, 2', 5, 5'-Tetrachlorobenzidine	15721-02-5	TCI America *via* NTP	A	6.25	Ames pos. (+S9), not tested by NTP	Insufficient data	IARC Monograph no. 27 (1982)
2, 3-Dibromopropionic acid	600-05-5	Sigma-Aldrich *via* NTP	A	203	Ames pos., no NTP data	Insufficient data	Søderlund et al. (1979)
2, 4-Bis(1-methyl-1-phenylethyl)phenol	2772-45-4	Sigma-Aldrich *via* NTP	A	49.7	No NTP data, no publications	Insufficient data	NA
2, 4-Di-tert-butylphenol	96-76-4	Sigma-Aldrich *via* NTP	A	99.5	No NTP data, no publications	Insufficient data	NA
2, 4-Diaminotoluene	95-80-7	Sigma-Aldrich *via* NTP	A	196	Ames pos. (+S9), *in vitro* CA and SCE pos., *in vivo* MN pos.	Positive	NTP (https://doi.org/10.22427/NTP-DATA-1); Leadscope
2, 6-Toluenediamine	823-40-5	Sigma-Aldrich *via* NTP	A	204	*in vitro* CA pos., *in vivo* MN pos.; NTP tested the dihydrochloride salt: *in vitro* CA pos., *in vivo* MN pos.	Positive	Leadscope; NTP
3-Butyl-1-nitro-3-nitrosoguanidine	13010-08-7	Sigma-Aldrich *via* NTP	A	72.1	Ames pos., not tested by NTP	Insufficient data	Leadscope

Table 1. (continued)

Chemical	CAS No.	Source	**Test Group**[a]	Top Conc. (μM)	Other Genetox[b]	Mammalian Cell Genetox Expectation[c] (-S9)	References and Miscellaneous Notes
3-Iodo-2-propynyl-N-butylcarbamate	55406-53-6	Sigma-Aldrich	A	6.21	No NTP data, no publications	Insufficient data	NA
3-Methoxycatechol	934-00-9	Sigma-Aldrich *via* NTP	A	74.8	No NTP data; genotoxic upon nitrosation	Insufficient data	Ohshima et al. (1989)
3-Phenylprop-2-enal (trans-Cinnamaldehyde)	14371-10-9	Sigma-Aldrich *via* NTP	A	101	Ames pos. (weak), *in vitro* SCE pos., *in vitro* CA pos. (although NTP study was neg.)	Positive	Leadscope; NTP
4-(Benzyloxy)phenol	103-16-2	Sigma-Aldrich *via* NTP	A	49.25	No NTP data, no publications	Insufficient data	NA
4-Methylcatechol	452-86-8	Sigma-Aldrich *via* NTP	A	24.4	Ames neg., *in vitro* CA pos., *in vivo* MN neg.	Positive	NTP; Leadscope; Stich et al. (1981)
4, 4'-Diaminoazobenzene	538-41-0	Acros Organics *via* NTP	A	102	Ames pos. (+S9), no NTP data	Insufficient data	Shahin (1989)
4, 4'-Thiodiphenol	2664-63-3	Sigma-Aldrich *via* NTP	A	189	No NTP data, no publications	Insufficient data	NA
6-Azacytidine	3131-60-0	RTI International *via* NTP	A	100	*in vitro* MN pos. (K-)	Positive	Stopper et al. (1995); nucleoside analog
6-Thioguanine	154-42-7	Sigma-Aldrich *via* NTP	A	3.09	Ames pos., *in vitro* CA pos., *in vivo* MN pos.	Positive	NTP; nucleoside analog
8-Hydroxyquinoline	148-24-3	Sigma-Aldrich *via* NTP	A	8.88	Ames pos., *in vitro* CA and MLA pos.	Positive	NTP
Adriamycin HCl (a.k.a. Doxorubicin HCl)	25316-40-9	Toronto Research Chemicals Inc. *via* NTP	A	0.2	Ames pos., *in vitro* CA pos., *in vivo* MN pos.	Positive	Leadscope; NTP; topoisomerase 2 inhibitor
Ampicillin trihydrate	7177-48-2	Sigma-Aldrich	A	1000	Ames neg., *in vitro* CA neg. (pos. at conc. higher than therapeutic plasma conc., *in vivo* MN neg.	Negative	Kirkland et al. (2016)
Anisomycin		Sigma-Aldrich	A	10	*in vitro* MN neg. with high levels of apoptosis	Negative	Maik Schuler, Richard Spellman, Maria Engel (personal communication); protein biosynthesis inhibitor
Apigenin	520-36-5	Sigma-Aldrich *via* NTP	A	49.7	Ames neg.	Insufficient data	NTP
AZD2858	486424-20-8	Selleckchem	A	49.98	*in vitro* CA and MN pos.	Positive	Personal communication, Ann Doherty; Glycogen Synthase Kinase-3 inhibitor

Table 1. (continued)

Chemical	CAS No.	Source	**Test Group**[a]	Top Conc. (μM)	Other Genetox[b]	Mammalian Cell Genetox Expectation[c] (-S9)	References and Miscellaneous Notes
Beta-Lapachone	4707-32-8	Selleckchem	A	100	*in vitro* CA and comet pos.	Positive	Degrassi et al. (1993), Vanni et al. (1998); Topoisomerase I inhibitor
Bis(1-piperidinylthioxomethyl) hexasulfide	971-15-3	Pfaltz & Bauer, Inc. *via* NTP	A	12.75	No NTP data, no publications	Insufficient data	NA
Bis[4-(glycidyloxy)phenyl]methane	3/6/95	Sigma-Aldrich *via* NTP	A	50.25	No NTP data, no publications	Insufficient data	NA
Bisphenol AF	1478-61-1	3B Scientific Corporation *via* NTP	A	70.7	Ames neg., *in vivo* MN neg	Insufficient data	NTP
Cadmium acetate dihydrate	4/4/43	ICN Biomedicals, Inc. *via* NTP	A	4.44	other Cd salts: *in vitro* MN, CA, and *Hprt* pos., *in vivo* CA and MN pos.	Positive	Kirkland et al. (2016)
Cadmium Cl	10108-64-2	Sigma-Aldrich *via* NTP	A	3.15	*in vitro* MN, CA, and *Hprt* pos., *in vivo* CA and MN pos.	Positive	Kirkland et al. (2016)
Chlorocholine chloride	999-81-5	Sigma-Aldrich	A	1000	Ames neg., *in vitro* CA neg, *in vivo* CA neg.	Negative	Kirkland et al. (2016)
Copper dimethyldithiocarbamate	137-29-1	TCI America *via* NTP	A	0.354	No NTP data; other soluble Cu compounds: *in vitro* SCE and *Hprt* pos.	Positive	Sideris et al. (1988)
Dasatinib	302962-49-8	Selleckchem	A	25	Ames neg., clastogenic when tested in CHO cells (±S9), *in vivo* MN neg.	Positive	Sprycel package insert (2010); tyrosine kinase inhibitor, especially Ber-Abl, Scr, c-Kit
Digitonin	11024-24-1	Sigma-Aldrich *via* NTP	A	6.34	Ames neg.	Insufficient data	NTP
Dodecyl gallate (lauryl gallate)	1166-52-5	Sigma-Aldrich *via* NTP	A	6.84	*in vitro* comet pos. (although aspects of this study not performed to current standards), no NTP data	Insufficient data	Savia et al. (2005)
Ethanamine, 2-chloro-N, N-diethyl-, HCl	869-24-9	Sigma-Aldrich *via* NTP	A	101	No NTP data, no publications	Insufficient data	NA
Gefitinib	184475-35-2	Sigma-Aldrich	A	25	*in vitro* and *in vivo* genetic toxicity neg.	Negative	Iressa package insert (2003); EGFR tyrosine kinase inhibitor
Genistein	446-72-0	Sigma-Aldrich *via* NTP	A	197	Ames pos. (+S9), *in vitro* CA pos.	Positive	NTP; Leadscope; topoisomerase 2 inhibitor

Table 1. (continued)

Chemical	CAS No.	Source	**Test Group**[a]	Top Conc. (μM)	Other Genetox[b]	Mammalian Cell Genetox Expectation[c] (-S9)	References and Miscellaneous Notes
Glutaraldehyde	111-30-8	Sigma-Aldrich *via* NTP	A	18	Ames pos., *in vitro* CA and MLA pos., *in vivo* MN neg. and equivocal	Positive	NTP
Hesperadin	422513-13-1	Selleckchem	A	0.25	*in vitro* MN pos., aberrant metaphases	Positive	Hauf et al. (2003) and Kurihara et al. (2006); Aurora B kinase inhibitor
Hydroquinone	123-31-9	Sigma-Aldrich *via* NTP	A	49.75	Ames pos. (although NTP study was neg.), *in vitro* CA pos. (although NTP study was only pos. +S9), *in vitro* MLA pos (± S9), *in vivo* MN pos.	Positive	Leadscope, NTP
Irinotecan	57852-57-0	Selleckchem	A	5	Ames neg., *in vitro* cytogenetics pos., *in vivo* MN pos.	Positive	Camptosar packet insert (2014); topoisomerase 1 inhibitor
Malachite green oxalate	2437-29-8	TCI America *via* NTP	A	0.25	Generally Ames neg. in absence of S9, *in vitro* CA neg., *in vivo* MN and *Hprt* neg.	Negative	NTP Toxicity Report Series No. 71 (2004), Au and Hsu (1979), and Mittelstaedt et al. (2004)
Menthol	89-78-1	Sigma-Aldrich	A	499.8	Ames neg., *in vitro* CA neg. and pos. reports, *in vitro* MN neg. in p53 competent human cells	Negative	Kirkland et al. (2016)
Mercuric chloride	7487-94-7	Sigma-Aldrich *via* NTP	A	6.22	Ames neg., *in vitro* CA pos., MLA pos.	Positive	NTP
Monocrotaline	315-22-0	Sigma-Aldrich *via* NTP	A	201	*in vitro* MN pos.; *in vivo* MN pos.	Positive	MacGregor et al. (1990) and Müller et al. (1992)
N-Phenyl-1, 4-benzenediamine HCl (a.k.a. p-anilinoaniline)	2198-59-6	Acros Organics *via* NTP	A	49.5	*in vitro* comet pos., no NTP data	Positive	Elliott and Reiners (2008)
Osimertinib	1421373-65-0	Selleckchem	A	7.8	*in vitro* and *in vivo* genetic toxicity neg.	Negative	Tagrisso, package insert (2012); EGFR kinase inhibitor
Oxiranemethanamine, N-[4-(oxiranylmethoxy)phenyl]-N-(oxiranylmethyl)-	5026-74-4	Sigma-Aldrich *via* NTP	A	12.5	No NTP data, no publications	Insufficient data	NA

Table 1. (continued)

Chemical	CAS No.	Source	**Test Group**[a]	Top Conc. (μM)	Other Genetox[b]	Mammalian Cell Genetox Expectation[c] (-S9)	References and Miscellaneous Notes
Palbociclib	827022-33-3	Sigma-Aldrich	A	12.49	Ames neg., *in vitro* and *in vivo* MN pos., *in vitro* MN shown to arise from aneugenic MoA, *in vitro* ChromAb neg.	Positive	Ibrance package insert (2015), Wu et al. (2015, personal communication), Zhanna Sobol; cyclin-dependent kinase inhibitor
Pentabromoethane	75-95-6	Supelco *via* NTP	A	142	Ames neg., no publications	Insufficient data	NTP
Pyrimethamine	58-14-0	Sigma-Aldrich *via* NTP	A	6.34	Ames neg., *in vitro* SCE and CA pos.	Positive	NTP
Resveratrol	501-36-0	ChromaDex, Inc. *via* NTP	A	202	*in vitro* clastogenesis	Positive	Basso et al. (2013), Fox et al. (2012), and Leone et al. (2012); topoisomerase 2 inhibitor
sec-Butylparaben	17696-61-6	TCI America *via* NTP	A	201	No NTP data, no publications	Insufficient data	NA
Selenious acid	7783-00-8	Sigma-Aldrich *via* NTP	A	100	*in vitro* comet pos., *in vitro* CA pos.	Positive	Cemeli et al. (2003) and Nakamuro et al. (1976)
Selenium dioxide	8/4/46	Sigma-Aldrich *via* NTP	A	102	*in vitro* SCE pos. (human lymphocytes)	Positive	Ray and Altenberg (1980)
Sesamol	533-31-3	Sigma-Aldrich *via* NTP	A	199	Ames neg., pro-oxidant at high conc.	Insufficient data	NTP; Khamphio et al. (2016)
Strobane	8001-50-1	Chem Service, Inc. *via* NTP	A	49.2	No NTP data, no publications	Insufficient data	NA
Tannic acid	1401-55-4	Santa Cruz Biotechnology, Inc. *via* NTP	A	72.3	*in vitro* CA and MN pos.	Positive	EFSA Journal (2014)
Tetraphenylolethane glycidyl ether	7328-97-4	Sigma-Aldrich *via* NTP	A	31.25	*in vitro* MN pos.	Positive	Nishihara et al. (2016)
Topiramate	97240-79-4	Sigma-Aldrich	A	1000	Ames neg., *in vitro* CA and MLA neg., *in vivo* CA neg.	Negative	Kirkland et al. (2016)
Tozasertib (a.k.a. VX-680)	639089-54-6	Selleckchem	A	1	*in vitro* MN pos. (primarily K+, also polyploidy)	Positive	Gollapudi et al. (2014); pan-Aurora kinase inhibitor, especially Aurora A
Tribromoacetaldehyde	115-17-3	Sigma-Aldrich via NTP	A	2.64	*in vitro* comet pos., *in vitro* MN neg.	Positive (owing to clear TK6 comet positive results with high levels of oxidized bases)	Jeong et al. (2015) and Liviac *et al.* (2010)

Table 1. (continued)

Chemical	CAS No.	Source	**Test Group**[a]	Top Conc. (μM)	Other Genetox[b]	Mammalian Cell Genetox Expectation[c] (-S9)	References and Miscellaneous Notes
Tributyltetradecylphosphonium Cl	81741-28-8	Cytec Industries Inc. *via* NTP	A	1	No NTP data, no publications	Insufficient data	NA
Tributyltetradecylphosphonium dodecylbenzenesulfonate	NOCAS_49391	IoLiTec Ionic Liquids Technologies Inc. *via* NTP	A	1	No NTP data, no publications	Insufficient data	NA
Tris (2-ethylhexyl) phosphate	78-42-2	Sigma-Aldrich	A	1000	Ames neg., *in vitro* CA neg., *in vivo* CA and MN neg.	Negative	Kirkland et al. (2016)
Zafirlukast	107753-78-6	Sigma-Aldrich	A	124.9	Ames neg., *in vitro* MLA, CA and *Hprt* neg.	Negative	Kirkland et al. (2016)
Zinc dibutyldithiocarbamate	136-23-2	TCI America *via* NTP	A	8.83	Ames neg., *in vitro* CA pos., *in vitro* MLA neg.	Positive	Matsuoka et al. (2005) and Tinklera *et al.* (1998)
Ziram	137-30-4	Sigma-Aldrich *via* NTP	A	0.177	Ames pos., *in vitro* CA pos.	Positive	NTP
ZM-447439	331771-20-1	Selleckchem	A	25	*in vitro* MN pos. (primarily K+, also polyploidy)	Positive	Gollapudi et al. (2014); Aurora kinase A/B inhibitor
1-Amino-2-methylanthraquinone	82-28-0	Sigma-Aldrich *via* NTP	S	99	Ames pos. (+S9); *in vitro* CA pos. (+S9, CHO cells), *in vitro* SCE pos. (± S9, CHO)	Insufficient data	NTP
2-Amino-5-azotoluene	97-56-3	Sigma-Aldrich *via* NTP	S	70.7	Ames pos. (+S9)	Insufficient data	NTP
2-Hydroxyanthraquinone	605-32-3	TCI America *via* NTP	S	70.7	Ames pos. (+S9, weak)	Insufficient data	REACH Monitor (2012)
3'-Methyl-4-dimethylaminoazobenzene	55-80-1	TCI America *via* NTP	S	21.7	Ames pos. (-S9, weak)	Insufficient data	Lefevre and Ashby (1981)
4-(Dimethylamino)azobenzene	60-11-7	Sigma-Aldrich *via* NTP	S	70.7	Ames pos. (+S9), *in vitro* MLA pos. (+S9), *in vivo* MN pos.	Negative	NTP; Leadscope
4-Azoxyanisole	1562-94-3	Sigma-Aldrich *via* NTP	S	17.49	Ames pos. (+S9)	Insufficient data	NTP
Biochanin A	491-80-5	Sigma-Aldrich *via* NTP	S	201	DNA adducts and aneuploidy in SHE cells without S9	Positive	Tsutsui et al. (2003)
Cyproterone acetate	427-51-0	Sigma-Aldrich *via* NTP	S	122.8	*in vitro* CA with metabolically competent cells, *in vivo* MN pos.	Insufficient data	Leadscope; Kasper *et al.* (2001)
D&C Yellow 11	8003-22-3	Sigma-Aldrich *via* NTP	S	35.7	Ames, *in vitro* CA pos.	Positive	NTP
N-Phenyl-1-naphthylamine	90-30-2	Sigma-Aldrich *via* NTP	S	101	Ames, *in vitro* CA neg.	Negative	NTP

Table 1. (continued)

Chemical	CAS No.	Source	**Test Group**[a]	Top Conc. (μM)	Other Genetox[b]	Mammalian Cell Genetox Expectation[c] (-S9)	References and Miscellaneous Notes
N, N'-Diphenyl-p-phenylenediamine	74-31-7	Sigma-Aldrich *via* NTP	S	35.3	Ames pos. (+S9), *in vitro* SCE pos. (±S9), *in vitro* CA pos. (although NTP study was neg.)	Positive	NTP; Leadscope
Phenethyl anthranilate	133-18-6	Sigma-Aldrich *via* NTP	S	201	Ames neg.	Insufficient data	NTP
Rosuvastatin calcium	147098-20-2	Sigma-Aldrich *via* NTP	S	707	Ames neg., *in vitro* MLA and CA neg.	Negative	Kirkland et al. (2016)
Saquinavir mesylate	149845-06-7	Roche Research Center *via* NTP	S	52.7	Ames, *in vitro* CA, *in vivo* MN neg.	Negative	Invirase package insert (2012); HIV protease inhibitor
1, 3-Dichlorobenzene	541-73-1	Sigma-Aldrich *via* NTP	I	199	*Escherichia coli* and *in vivo* MN pos., NTP Ames neg.	Positive	EPA, toxicological review of dichlorobenzenes (2006); NTP
2-Amino-6-methoxybenzothiazole	1747-60-0	Sigma-Aldrich *via* NTP	I	71	Ames pos. (+S9), *in vitro* CA pos. (much stronger with S9), *in vitro* MLA pos. (+S9), *in vivo* MN pos. in female mice, *in vivo* MN neg. in male mice	Negative	NTP
2-Butoxyethanol	111-76-2	Sigma-Aldrich *via* NTP	I	200	Ames neg., *in vitro* SCE and CA neg.; *in vivo* MN neg.	Negative	NTP
2-Methoxy-5-methylaniline (a.k.a. p-Cresidine)	120-71-8	Sigma-Aldrich *via* NTP	I	194	Ames pos. (+S9), *in vitro* CA pos. (+S9, weak), *in vivo* MN pos.; NTP study was neg.	Negative	Leadscope; NTP
9, 10-Dihydrobenzo[a]pyrene-7(8H)-one	3331-46-2	Sigma-Aldrich *via* NTP	I	191	No NTP data, no publications	Insufficient data	NA
Acetic acid, mercapto-, monoammonium salt	5421-46-5	TCI America *via* NTP	I	201	No NTP data, no publications	Insufficient data	NA
Black cohosh extract	84776-26-1	Frutarom Switzerland Ltd. *via* NTP	I	25	*in vitro* MN pos., *in vivo* MN pos.	Positive	NTP; Mercado-Feliciano et al. (2012)
C.I. Basic Orange 2	532-82-1	Sigma-Aldrich *via* NTP	I	197	Ames pos. (+S9)	Insufficient data	NTP
Daidzein	486-66-8	Sigma-Aldrich *via* NTP	I	198	Ames neg., *in vitro* CA neg.	Negative	NTP; Leadscope
Dimethylsulfoxide	67-68-5	Gaylord Chemical Company, LLC *via* NTP	I	1% v/v	Ames neg., *in vitro* CA neg.	Negative	Common solvent, not expected to cause in vitro genotoxicity at conc. tested

Table 1. (continued)

Chemical	CAS No.	Source	**Test Group**[a]	Top Conc. (μM)	Other Genetox[b]	Mammalian Cell Genetox Expectation[c] (-S9)	References and Miscellaneous Notes
Metronidazole	443-48-1	Sigma-Aldrich *via* NTP	I	205	Ames pos. (± S9), *in vitro* CA pos., *in vivo* MN pos.	Positive	NTP; Leadscope
Resorcinol	108-46-3	Sigma-Aldrich *via* NTP	I	195	Some pos. findings such as *in vitro* CA pos. (CHO), but generally neg. in p53-competent cel lines	Negative (in p53 competent cells)	Kirkland et al. (2016) and Stich et al. (1981)
Sorbic acid	110-44-1	Sigma-Aldrich via NTP	I	199	Ames neg.; *in vitro* CA, *in vivo* MN pos.	Positive	Leadscope; NTP
Thiocarbazide	2231-57-4	Alfa Aesar *via* NTP	I	205	Ames neg.	Insufficient data	Leadscope
Vinpocetine	42971-09-5	Maypro Industries, LLC *via* NTP	I	100	Ames neg., *in vivo* MN neg., *in vivo* comet stomach neg., blood neg., liver equivocal	Insufficient data	NTP

[a]Test Group A: adequately tested, either positive by at least 1 analysis method, or if negative tested to limit conc. or approached/achieved cytotoxicity limit, n = 74; Group S: top concentration limited by solubility (in DMSO), n = 14. Group I: inadequately tested, negative result and did not approach or achieve cytotoxicity limit, and did not reach limit conc. or solubility limit, n = 15.
[b]Unless otherwise stated Ames and *in vitro* mammalian cell results refer to test conditions in the absence of exogenous metabolic activation.
[c]Insufficient means an expected *in vitro* mammalian cell genotoxicity call cannot be made at this time for lack of sufficient conventional genotoxicity data.

solubility limit, and the assay's cytotoxicity limit was not approached (ie, nuclei count at 24 h did not reach 60% reduction relative to mean solvent control).

Cell culture and treatments. TK6 cells were purchased from ATCC (Manassas, VA; cat. no. CRL-8015). Cells were grown in a humidified atmosphere at 37 °C with 5% CO_2, and were maintained at or below 1×10^6 cells/ml. The culture medium consisted of RPMI 1640 and 200 μg/ml sodium pyruvate (both from Sigma-Aldrich, St. Louis, Missouri), 200 μM L-glutamine, 50 U/ml penicillin and 50 μg/ml streptomycin (from Mediatech Inc., Manassas, Virginia), and 10% v/v heat-inactivated horse serum (Gibco, a Thermo Fisher Scientific Company, Waltham, Massachusetts).

Chemicals selected by Litron scientists were tested using the same experimental design described previously in Bryce *et al.* (2016). Briefly, treatments occurred in U-bottom 96-well plates, with 198 μl TK6 cell suspension (2×10^5/ml) combined with 2 μl of DMSO-solubilized test chemical per well. The highest concentration tested was 1 mM, and the 19 additional concentrations were tested using a square root dilution scheme—ie, each concentration differed from the one above by a factor of 70.71%. In this manner a wide range of concentrations were evaluated (ie, nearly 3 orders of magnitude, 0.0014–1 mM). Each of the 20 concentrations was tested in a single well, whereas solvent was evaluated in 4 replicate wells. Upon addition of test chemical the plates were immediately incubated in a humidified atmosphere at 37 °C with 5% CO_2.

The NTP chemicals were tested similarly, with the following exceptions. Preliminary dose-range finding experiments were used to generate 24 h RNC data for each chemical provided (*via* MultiFlow—Cleaved PARP Kit, Rochester, New York; data not shown). Concentrations for the definitive experiment were chosen based on the RNC results with the intention to test at least 1 concentration that approached or slightly exceeded the assay's cytotoxicity limit, that is 80% reduction to RNC at 24 h (Bryce *et al.*, 2016). For the definitive experiments, 10 concentrations of each chemical were tested in duplicate wells of a 96-well plate. As described earlier, a square root 2 dilution scheme was used, except in the case of saquinavir mesylate, N-phenyl-1-naphthylamine, tetraphenylolethane glycidyl ether, malachite green oxalate, phenethyl anthranilate, tribromoacetaldehyde, 3-methoxycatechol, tannic acid, 3-iodo-2-propynyl-n-butylcarbamate, cyproterone acetate, and menthol. These chemicals demonstrated steep cytotoxicity curves, and for these agents, concentrations were more closely spaced (ie, each successive concentration was 85% of former, except for menthol, which differed by a factor of 90%).

DNA damage assay. TK6 cells were prepared for analysis using reagents and instructions included in MultiFlow DNA Damage Kit—p53, γH2AX, Phospho-Histone H3 (Litron Laboratories, Rochester, NY). The working solution, prepared fresh each day before use, was used to simultaneously digest cytoplasmic membranes, stain chromatin with a fluorescent nucleic acid dye, and label several nuclear epitopes with fluorescent antibodies. Anti-γH2AX-Alexa Fluor 647 was used to detect DNA double strand breaks, and antiphospho-histone H3-PE served as a mitotic cell marker. Antip53-FITC was used to label nuclear-localized p53, a subcellular translocation event that occurs in response to diverse genotoxicants. Included in the working solution were RNase plus propidium iodide to label nuclei and to facilitate detection of polyploidization, and counting beads in order to calculate nuclei densities (Sphero Multi-Fluorophore Particles, cat. no. FP-3057-2; Spherotech, Inc., Lake Forest, Illinois).

At the 4 and 24 h sampling times, cells were resuspended with pipetting, then 25 μl were removed from each well and added to a new 96-well plate containing 50 μl/well of prealiquoted working MultiFlow reagent solution. Mixing was accomplished by pipetting the contents of each well several times. After incubation at room temperature for 30 min, flow cytometric analysis was carried out as described below.

Flow cytometric analysis. Flow cytometric analysis was carried out using either a FACSCanto II flow cytometer equipped with a BD High Throughput Sampler or a Miltenyi Biotec MACSQuant Analyzer 10 flow cytometer with integrated 96-well MiniSampler device. Stock photomultiplier tube detectors and associated optical filter sets were used to detect fluorescence emissions associated with the fluorochromes: FITC (detected in the FITC channel, to use BD instrument parlance), PE (PE channel), propidium iodide (PerCP-Cy5.5 channel), and Alexa Fluor 647 (APC channel). Generally speaking, 4 h samples provided approximately 1000 nuclei for analysis with $>$ 2n DNA content, and 24 h samples provided 1000–4000 $\geq$ 2n nuclei.

Representative bivariate graphs, gating logic, and position of regions have been described in detail in earlier reports (Bernacki *et al.*, 2016; Bryce *et al.*, 2016, 2017). Briefly, 2 biomarker measurements, γH2AX and p53, were based on median fluorescence intensities, and these values were converted to fold-change by dividing them by the mean value associated with solvent-exposed cultures on the same plate. Polyploidy and p-H3 biomarker measurements were based on their frequency among other cells, and these values were converted to fold-change by dividing them by the mean value associated with solvent-exposed cultures on the same plate. Nuclei to counting bead ratios were calculated for each sample, and these ratios were used to determine absolute nuclei counts (those with 2n and greater DNA-associated propidium iodide fluorescence). Nuclei counts were used in turn to derive RNC. %Cytotoxicity was calculated as 100% minus %RNC at 24 h.

Machine learning models: general strategy. Several machine learning tools were studied, and they are described in detail in the subsequent section. General information shared across the 3 approaches is provided here. (For additional information, interested readers may consult Fundamentals of Predictive Analytics with JMP, 2nd Edition, Klimberg and McCullough, 2016). Multinomial LR, artificial neural network (ANN), and random forest (RF) models were built with JMP Pro software for Macintosh (v13, SAS Institute, Cary, North Carolina). These various models utilized 4 and 24 h MultiFlow data with the goal of predicting whether a chemical exhibits genotoxic activity or not, and if present whether the genotoxicity occurs *via* a clastogenic, aneugenic, or clastogenic and aneugenic ("mixed") MoA. The models were trained and optimized based on a set of 85 previously studied chemicals for which clastogenic, aneugenic, or nongenotoxic labels were specified (Bryce *et al.*, 2016, 2017). Supplementary Material 1 provides results from RF analysis that ranked variable importance that is the relative value of 10 MultiFlow assay biomaker/time point combinations, in terms of their ability to discriminate training set chemicals according to their specified MoA: clastogenic, aneugenic, nongenotoxic. Combinations of the 7 most predictive biomarker/time point were used in the optimized models described below.

Figure 1 depicts the overall scheme, whereby LR, ANN, and RF models were built and cross validated with training set data,

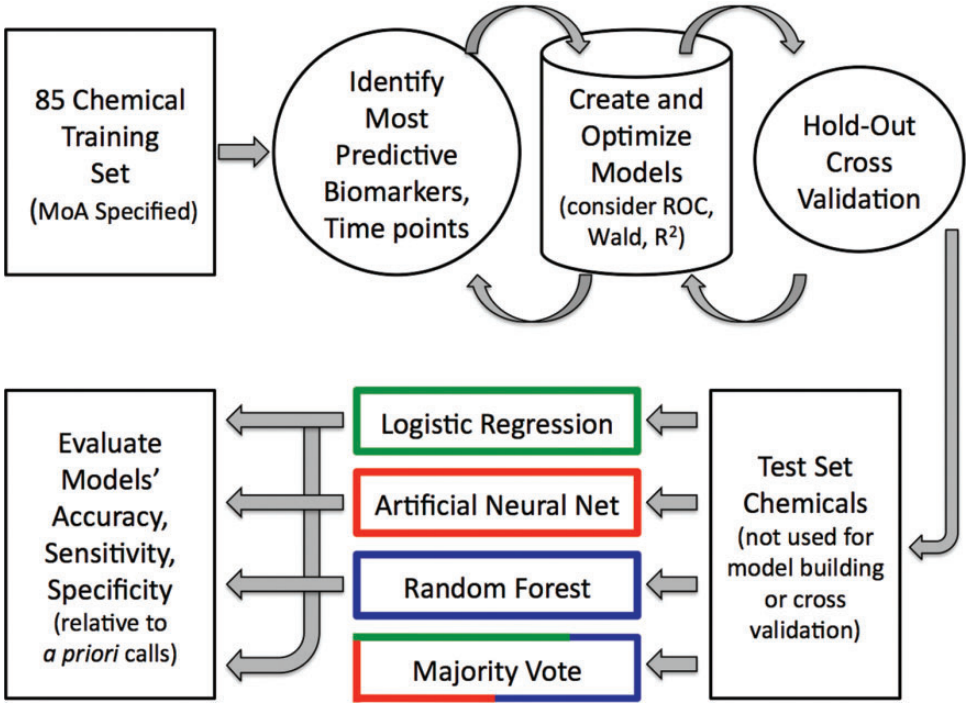

Figure 1. Overview of the several machine learning approaches used to synthesize MultiFlow assay biomarker response data into *in vitro* mammalian cell genotoxic activity predictions.

and finally evaluated with an external test set, ie, the chemicals listed in Table 1. As shown in Figure 1, in addition to assessing the performance of the individual models, a majority vote ensemble was also considered (described in more detail below).

Each model's output was synthesized into a final call regarding genotoxic MoA by considering clastogen and aneugen probability scores as follows:

- genotoxic, with evidence for a clastogenic MoA, required 2 successive concentrations to exhibit clastogen probability scores $\geq$ 80%, or 1 concentration to exhibit a clastogen probability score $\geq$ 90%;
- genotoxic, with evidence for an aneugen MoA, required 2 successive concentrations to exhibit aneugen probability scores $\geq$ 80%, or 1 concentration to exhibit an aneugen probability score $\geq$ 90%; and
- nongenotoxic was defined as the absence of 2 successive concentrations exhibiting clastogen or aneugen probability scores $\geq$ 80%, and no 1 concentration exhibiting a clastogen or aneugen probability score $\geq$ 90%.

The majority vote ensemble considered the genotoxicity calls from each of the 3 modeling approaches—LR, ANN, and RF—as described earlier. For this strategy, a simple majority (2 out of 3) was necessary for a genotoxic call.

Note that it is possible for the prediction algorithms to generate clastogen and aneugen probability scores that exceed the thresholds noted above for the same one chemical. This can occur at the same overlapping concentration(s), or at nonoverlapping concentration(s). In either of these cases the chemical was considered genotoxic with evidence for both clastogenic and aneugenic MoA.

LR, ANN, and RF. Two LR models were developed. The first, a clastogen-detection model, was based on fold-change data obtained for the following 4 clastogen-sensitive biomarkers: 4 h gH2AX, 4 h p53, 24 h gH2AX, and 24 h p53. As described in Bryce *et al.* (2017), in order to normalize the responses across the diverse set of training chemicals, and to give results stemming from higher exposures greater significance, the LR platform's weight function was used, specifically the variable %cytotoxicity at 24 h. The resulting model's algorithm provided probability scores for a clastogenic MoA at every concentration evaluated. The same strategy was used to construct a LR aneugen-detection model, which was based on the fold-change data obtained for the following 4 aneugen-sensitive biomarkers: 4 h p-H3, 24 h p-H3, 24 h polyploidy, and 24 h p53. Again, a weight function was applied using the variable 24 h %cytotoxicity. The resulting algorithm provided probability scores for an aneugenic MoA at every concentration evaluated.

Two ANN models were developed. The first, a clastogen-detection model, was based on the fold-change data obtained for the following 4 clastogen-sensitive biomarkers: 4 h γH2AX, 4 h p53, 24 h γH2AX, and 24 h p53. One hidden layer was specified, and the model utilized 3 *tanh* activation nodes. The resulting algorithm provided probability scores for a clastogenic MoA at every concentration evaluated. The same strategy was used to construct an aneugen-detection ANN model, and this was based on the fold-change data obtained for the following 4 aneugen-sensitive biomarkers: 4 h p-H3, 24 h p-H3, 24 h polyploidy, and 24 h p53. One hidden layer was specified, and the model utilized 3 *tanh* activation nodes. The resulting algorithm provided probability scores for an aneugenic MoA at every concentration evaluated. Note that in the case of ANN, model tuning included transformation of 24 h polyploidy fold-increase values. More specifically, square root transformation provided polyploidy dynamic range that more closely matched the other biomarkers, and it increased R^2, receiver operating characteristic values, and other performance metrics.

One RF model was developed based on the fold-change data obtained for the following 7 clastogen- and aneugen-responsive biomarkers: 4 and 24 h γH2AX, 4 and 24 h p53, 4 and 24 h p-H3, and 24 h polyploidy. The RF was comprised of 300 trees, with 3

of the 7 explanatory factors randomly chosen per split. A weight function was applied using the variable 24 h %cytotoxicity. The resulting algorithm provided probability scores for a clastogenic and aneugenic MoA at every concentration evaluated.

Performance assessments. Performance assessments of the MultiFlow assay were limited to the subset of A and S chemicals with enough conventional genotoxicity data to derive expert-based calls regarding their *in vitro* mammalian cell genotoxicity potential (n = 54). This facilitated calculation of accuracy values, ie, the percentage of correct calls regarding chemicals' *in vitro* genotoxic potential. Thus, MultiFlow results that provided sufficiently high clastogen and/or aneugen probability scores were considered correct for presumed genotoxicants and absence of high clastogenic and/or aneugenic probabilities were correct for presumed nongenotoxicants. These results were also used to calculate sensitivity and specificity values. Additional information regarding genotoxicity MoA predictions accompanied these primary calls that focused on presence or absence of genotoxic potential. As described earlier and illustrated by Figure 1, these secondary assessments were made for each of the machine learning models investigated.

RESULTS AND DISCUSSION

Prototypicals

Three chemicals that produced prototypical response profiles are described in detail to illustrate the type of data generated by the MultiFlow DNA Damage assay. The profiles include dose-response relationships for each individual biomarker at each of 2 time points. These examples should provide a useful background for interpreting the aggregate chemical results that are presented hereafter.

Anisomycin-exposed TK6 cells demonstrated a characteristic nongenotoxicant response profile (Figure 2A[AQ9]). The compound is clearly cytotoxic as evidenced by a dose-dependent reduction to %RNC. Even at concentrations that approached the assay's cytotoxicity limit, no substantial increases to p-H3, p53 or polyploidization biomarkers were observed. At the highest concentration tested (10 μM), a modest increase in γH2AX was evident, but only at the 24 h time point. Even so, none of the machine learning models generated high clastogen or aneugen probability scores. This pattern illustrates the way the current models, based on an 85 chemical training set, tend to behave. That is, a single modestly elevated endpoint at one time point is insufficient to trigger a genotoxicant call. Rather, as described in Bryce *et al.* (2017) and confirmed by computer simulations (data not shown), responses for 2 or more endpoints and/or time points are generally required to produce sufficiently high probability scores for genotoxicity.

Treatment of TK6 cells with adriamycin HCl resulted in a clastogenic response profile (Figure 2B). Whereas γH2AX and p53 biomarkers were increased at both the 4 and 24 h time points, there was no change to polyploidy, and the p-H3 biomarker was reduced in a dose-dependent manner. Regarding γH2AX and p53 responses, lower concentrations were more effective at the 24 h time point compared with the 4 h time point. This is a typical finding for clastogenic agents, although variability is seen in the degree by which these responses shift to lower effective concentrations with increasing treatment time. As shown by the predictive analytics output (Figure 2B), each of the models identified adriamycin as genotoxic, with evidence for a clastogenic MoA.

As indicated in Table 1, 2,2', 5,5'-tetrachlorobenzidine has not been studied sufficiently in conventional genotoxicity assays to form an *a priori* expectation about its potential to damage DNA. Even so, MultiFlow response data are instructive because they illustrate a typical aneugenic response profile (Figure 2C). Thus, while γH2AX did not increase at either time point and p53 translocation was not apparent at 4 h, marked p53 responses were observed at 24 h. Furthermore, marked increases in p-H3 positive events were induced by 2,2', 5,5'-tetrachlorobenzidine, and this was accompanied by evidence of polyploidization. It is therefore not surprising that each of the machine learning models identified this compound as genotoxic, with evidence for an aneugenic MoA.

Aggregate

As exemplified by Figures 2A–2C, each of the 103 test chemicals was evaluated over a wide range of concentrations for activity measured by several multiplexed biomarkers at 2 time points, and 3 machine learning approaches were used to generate aneugen and clastogen probability scores. This scheme generated 16 410 data points in total. The volume of data imposed constraints upon the level of detail that could be provided for individual chemicals, and it also reinforced the need for data analytics and visualization strategies that could keep pace with the rate by which MultiFlow data are acquired.

LR, ANN, and RF models provided rapid and streamlined approaches for meeting the data analysis requirements of this multiplexed assay. Given the nature of the models' output (clastogen and aneugen probability scores for each concentration tested), we found Manhattan plots to be one effective way of synthesizing and visualizing the aggregate results. Figure 3 shows probability score graphs resulting from the clastogen and aneugen ANN models (panels A and B, respectively). Although dose-response information is lost, the main advantages to this approach are that it is readily executed in the JMP program, and it effectively relates how each of 103 chemicals behaved in the MultiFlow assay. The clastogen and aneugen probability scores produced by the LR and RF models are provided in the same graphical format, and appear as Supplementary Materials 2 and 3.

Figure 3 clearly demonstrates that the compound set provided by the NTP included a high percentage of genotoxic agents. It is also apparent that the majority of the genotoxicants were clastogens, whereas compounds showing the aneugenic MoA were relatively rare. This explains why the compounds chosen by Litron scientists to supplement the NTP-supplied chemicals included a number of nongenotoxicants and aneugenic agents that had not been tested with the MultiFlow assay previously.

Figure 4 depicts how each of the 3 machine learning methods, as well as an ensemble of these models, judged the genotoxic activity of each of the 103 chemicals. Whereas the majority of chemicals (87.5%) showed consistent positive or negative calls across all 4 data analysis strategies, some differences in performance were observed. These differences resulted in a range of accuracy values: 79.6% for RF, 89.9% for LR, and 90.7 for ANN. The ensemble provided moderate improvements. As shown in Figure 4, the majority vote strategy produced accuracy, specificity, and sensitivity values of 92.6%, 92.9%, and 92.5%, respectively.

For each chemical judged to be genotoxic, Figure 4 provides the associated genotoxic MoA prediction. Consistent with the ANN output shown in Figure 3A, each of the machine learning strategies predicted a clastogenic MoA for the majority of the chemicals tested. Exceptions included the several kinase

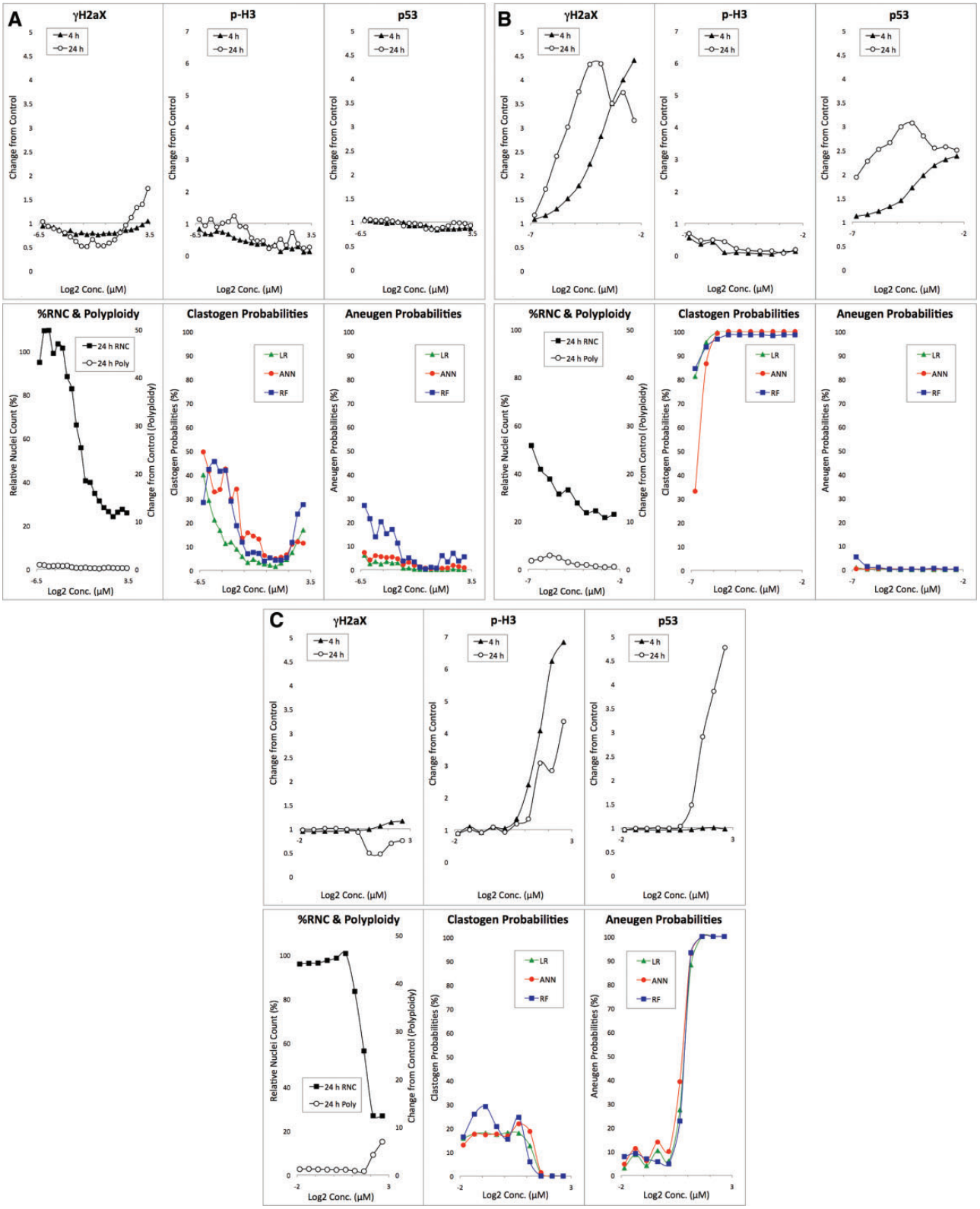

Figure 2. A, Biomarker response data are graphed for anisomycin-exposed TK6 cells versus concentration. The bottom middle panel shows clastogen probabilities as a function of anisomycin concentration based on 3 machine learning algorithms: LR, ANN, and RF. The bottom right panel shows analogous aneugen probability scores. B, Biomarker response data are graphed for adriamycin HCl-exposed TK6 cells versus concentration. The bottom middle panel shows clastogen probabilities as a function of adriamycin concentration based on 3 machine learning algorithms: LR, ANN, and RF. The bottom right panel shows analogous aneugen probability scores. C, Biomarker response data are graphed for 2,2', 5,5'-tetrachlorobenzidine-exposed TK6 cells versus concentration. The bottom middle panel shows clastogen probabilities as a function of 2,2', 5,5'-tetrachlorobenzidine concentration based on 3 machine learning algorithms: LR, ANN, and RF. The bottom right panel shows analogous aneugen probability scores.

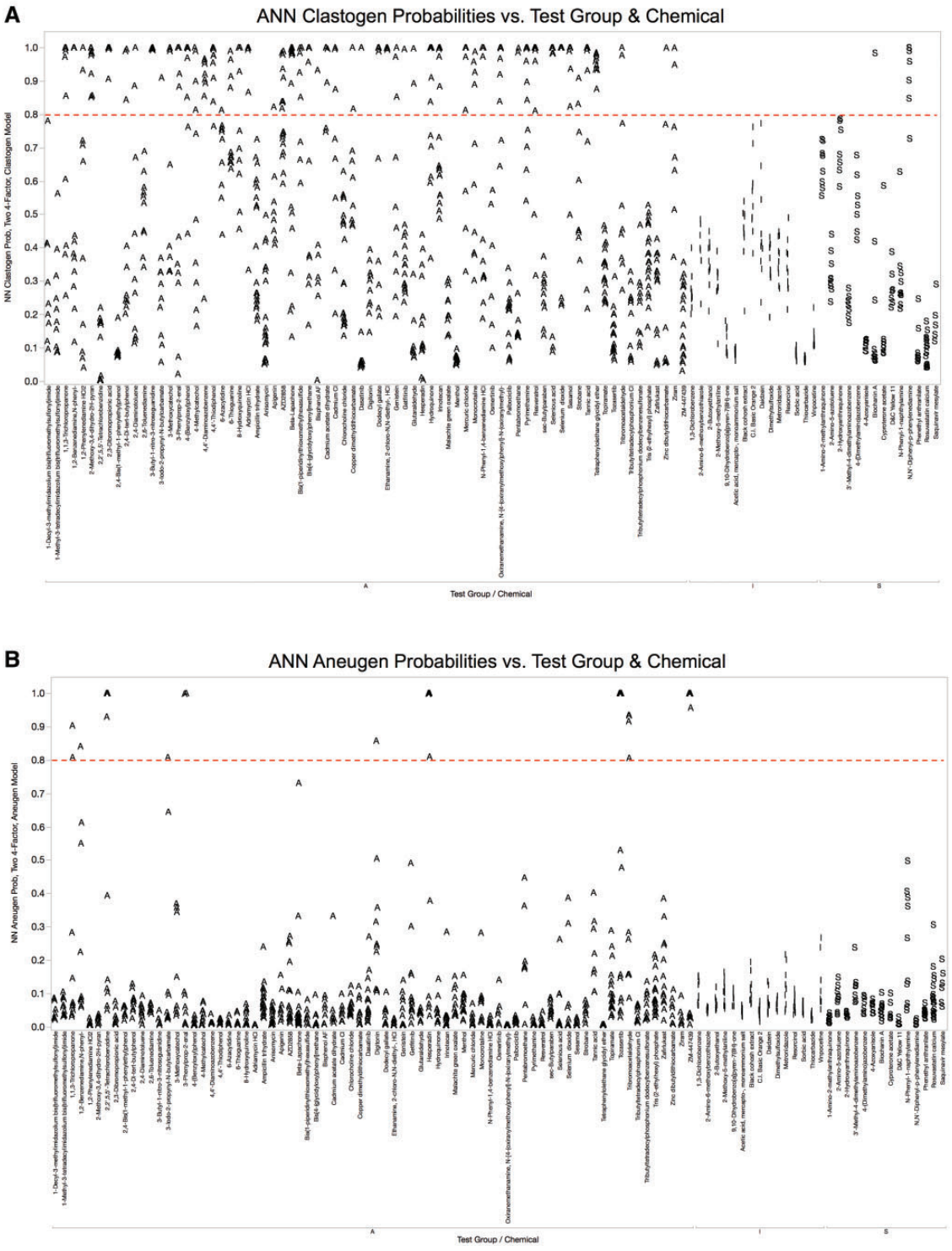

Figure 3. A, ANN probabilities for clastogen classification are graphed for each of 103 chemicals that were evaluated in TK6 cells with the MultiFlow DNA Damage assay. Chemicals are grouped according to class: A, adequately tested; I, inadequately tested; S, top concentration limited by solubility. A series of probabilities are plotted for each chemical, with each point representing a different concentration. A dashed line indicates the threshold value that probability scores had to reach in order to be considered significant. B, ANN probabilities for aneugen classification are graphed for each of 103 chemicals that were evaluated in TK6 cells with the MultiFlow DNA Damage assay. Chemicals are grouped according to class: A, adequately tested; I, inadequately tested; S, top concentration limited by solubility. A series of probabilities are plotted for each chemical, with each point representing a different concentration. A dashed line indicates the threshold value that probability scores had to reach in order to be considered significant.

inhibitors that supplemented the NTP chemical set. In any event, when considering the aggregate test set, whenever 2 or more models made a positive call for genotoxicity, they agreed on MoA 92.5% of the time. The exceptions included chemicals that may have been operating through both modes of action. This is discussed further, below.

Chemical	Test Group	Genotoxicity Expectation	Machine Learning Model Predictions			
			LR	ANN	RF	Majority Vote
1-Decyl-3-methylimidazolium bis(trifluoromethylsulfonyl)imide	A					
1-Methyl-3-tetradecylimidazolium bis(trifluoromethylsulfonyl)imide	A					
1,1,3-Trichloropropanone	A		C	C / A	C	C
1,2-Benzenediamine,N-phenyl-	A		C	C		C
1,2-Phenylenediamine HCl2	A		C	C	C	C
2-Methoxy-3,4-dihydro-2H-pyran	A		C	C	C	C
2,2',5,5'-Tetrachlorobenzidine	A		A	A	A	A
2,3-Dibromopropionic acid	A		C	C	C	C
2,4-Bis(1-methyl-1-phenylethyl)phenol	A					
2,4-Di-tert-butylphenol	A			C	C	C
2,4-Diaminotoluene	A		C	C	C	C
2,6-Toluenediamine	A				C	
3-Butyl-1-nitro-3-nitrosoguanidine	A		C	C	C	C
3-Iodo-2-propynyl-N-butylcarbamate	A					
3-Methoxycatechol	A		C	C	C	C
3-Phenylprop-2-enal (trans-Cinnamaldehyde)	A		C / A	C / A	C	C / A
4-(Benzyloxy)phenol	A		C	C	C	C
4-Methylcatechol	A		C	C	C	C
4,4'-Diaminoazobenzene	A			C		
4,4'-Thiodiphenol	A		C	C	C	C
6-Azacytidine	A		C		C	C
6-Thioguanine	A		C	C		C
8-Hydroxyquinoline	A		C	C	C	C
Adriamycin HCl	A		C	C	C	C
Ampicillin trihydrate	A					
Anisomycin	A					
Apigenin	A		C			
AZD2858	A		C	C	C	C
Beta-Lapachone	A		C	C	C	C
Bis(1-piperidinylthioxomethyl)hexasulfide	A		C	C	C	C
Bis[4-(glycidyloxy)phenyl]methane	A		C	C	C	C
Bisphenol AF	A			C		
Cadmium acetate dihydrate	A		C	C		C
Cadmium Cl	A		C	C		C
Chlorocholine chloride	A					
Copper dimethyldithiocarbamate	A		C	C	C	C
Dasatinib	A		C	C	C	C
Digitonin	A					
Dodecyl gallate (lauryl gallate)	A		C	C	C	C
Ethanamine, 2-chloro-N,N-diethyl-, HCl	A		C	C	C	C
Gefitinib	A		C	C	C	C
Genistein	A		C	C	C	C
Glutaraldehyde	A			C	C	C
Hesperadin	A		C / A	A		A
Hydroquinone	A		C	C	C	C
Irinotecan	A		C	C	C	C
Malachite green oxalate	A					
Menthol	A					
Mercuric chloride	A		C	C	C	C
Monocrotaline	A		C	C	C	C
N-Phenyl-1,4-benzenediamine HCl	A		C	C	C	C
Osimertinib	A				C	
Oxiranemethanamine, N-[4-(oxiranylmethoxy)phenyl]-N-(oxiranylmethyl)-	A		C	C	C	C
Palbociclib	A					
Pentabromoethane	A		C	C	C	C
Pyrimethamine	A		C	C	C	C
Resveratrol	A		C	C	C	C
sec-Butylparaben	A					
Selenious acid	A		C	C	C	C
Selenium dioxide	A		C	C	C	C
Sesamol	A		C	C	C	C
Strobane	A		C	C	C	C
Tannic acid	A		C	C		C
Tetraphenylolethane glycidyl ether	A		C	C	C	C
Topiramate	A					
Tozasertib	A		A	A	A	A
Tribromoacetaldehyde	A		C	C / A		C
Tributyltetradecylphosphonium Cl	A					
Tributyltetradecylphosphonium dodecylbenzenesulfonate	A					
Tris (2-ethylhexyl) phosphate	A					
Zafirlukast	A					
Zinc dibutyldithiocarbamate	A		C	C		C
Ziram	A		C	C	C	C
ZM-447439	A		A	A	A	A
1-Amino-2-methylanthraquinone	S		C			
2-Amino-5-azotoluene	S					
2-Hydroxyanthraquinone	S					
3'-Methyl-4-dimethylaminoazobenzene	S					
4-(Dimethylamino)azobenzene	S					
4-Azoxyanisole	S					
Biochanin A	S			C	C	C
Cyproterone acetate	S					
D&C Yellow 11	S					
N-Phenyl-1-naphthylamine	S					
N,N'-Diphenyl-p-phenylenediamine	S		C	C	C	C
Phenethyl anthranilate	S					
Rosuvastatin calcium	S					
Saquinavir mesylate	S					
1,3-Dichlorobenzene	I					
2-Amino-6-methoxybenzothiazole	I					
2-Butoxyethanol	I					
2-Methoxy-5-methylaniline (a.k.a. p-Cresidine)	I					
9,10-Dihydrobenzo[a]pyrene-7(8H)-one	I					
Acetic acid, mercapto-, monoammonium salt	I					
Black cohosh extract	I					
C.I. Basic Orange 2	I					
Daidzein	I					
Dimethylsulfoxide	I					
Metronidazole	I					
Resorcinol	I					
Sorbic acid	I					
Thiocarbazide	I					
Vinpocetine	I					
		Accuracy (%):	89.9	90.7	79.6	92.6
		Specificity (%):	92.9	92.9	85.7	92.9
		Sensitivity (%):	87.5	90.0	77.5	92.5

Figure 4. Information on 103 chemicals including expected and observed *in vitro* mammalian cell genotoxicity results is provided. Chemicals are grouped according to class: A, adequately tested; S, top concentration limited by solubility; I, inadequately tested. White cells in the "Genotoxicity Expectation" column indicate there is too little conventional genotoxicity data to form an opinion about DNA damage potential; yellow cells (gray in print version) denote a nongenotoxic expectation, and blue cells (black in print version) indicate an expectation of *in vitro* genotoxic activity in the absence of metabolic activation. Observed results are provided in the 4 rightmost columns and are based on MultiFlow assay data in conjunction with LR, ANN, and RF models, as well as a majority vote ensemble. In these columns white cells indicate that no call could be made due to inadequate testing (stock chemical concentration provided was too low); yellow cells (gray in print version) indicate a negative result; and blue cells (black in print version) denote a positive call. Note that when a genotoxic call was made, the following abbreviations indicate the predicted MoA: C, clastogen, A, aneugen, C/A, evidence of both. The performance metrics shown at the bottom are based on A and S class chemicals with a negative or positive genotoxicity expectation (n = 54).

Atypicals

Having described prototypical chemicals as well as aggregate results, several atypical response profiles are worth noting. Figure 5A shows individual biomarker response data and predictive analytics results for 6-thioguanine-exposed TK6 cells. As shown for the classic genotoxicant adriamycin, the vast majority of clastogens tested to date exhibit increased γH2AX levels at both the 4 and 24 h sampling times, often accompanied by marked p53 responses at both time points. In the case of 6-thioguanine, these 2 biomarkers were unresponsive at the early time point, with marked increases evident only at 24 h. The γH2AX dose-response relationship was also unusual in that after an initial increase, it proceeded to fall off at higher concentrations, even as p53 continued to rise. Whether aspects of this atypical response profile have the potential to serve as a signature of nucleoside analogs as a class will be worth further investigation. Preliminary support for this hypothesis comes from results for 6-azacytidine, which also exhibited late, not early, γH2AX and p53 increases.

As demonstrated by Bryce *et al.* (2015, 2016), Khoury *et al.* (2016), and Cheung *et al.* (2015), tubulin-binding aneugens generally cause robust p-H3 increases, often at both early and late time points. Although ZM-447439 is aneugenic (Gollapudi *et al.*, 2014), it caused drastic reductions to the p-H3 biomarker (Figure 5B). Two other aneugenicity signatures—late p53 increases and remarkable polyploidization—enabled each of the machine learning models to detect the agent's genotoxic potential and correctly ascribe it to an aneugenic MoA. This unusual response profile may be useful for differentiating aneugens that target certain kinases, perhaps especially those that inhibit 1 or more aurora kinases, since ZM-447439 is known to be a potent inhibitor of aurora kinase A and B (Baldini *et al.*, 2013). Preliminary support for this hypothesis comes from results for tozasertib (VX-680), a pan-aurora kinase inhibitor, and hesperadin, a potent inhibitor of aurora kinase B. In both of these cases, p-H3 was greatly reduced at 4 h, while p53 and polyploidy were highly elevated at 24 h.

Tribromoacetaldehyde has been described as producing positive results in an *in vitro* comet assay (TK6 cells) with evidence for high levels of oxidized bases, even though it failed to significantly induce micronuclei in these same cells (Liviac *et al.*, 2009). The authors ascribed failure to induce micronuclei to rapid and effective DNA repair. Figure 5C shows MultiFlow biomarker results for tribromoacetaldehyde. γH2AX and p53 responses are relatively modest, but combine to provide evidence of clastogenicity. On the other hand, robust dose-related increases in the p-H3 biomarker were observed, an indicator of aneugenicity. The 3 models' probability scores are interesting given these competing signals. Both the LR and ANN models interpreted the response profiles as evidence for clastogenicity, based on the γH2AX and p53 signals, and the ANN model further recognized the marked p-H3 increases as evidence of aneugenicity, suggesting a dual MoA. The RF model, on the other hand, did not identify tribromoacetaldehyde as genotoxic. Whereas the LR and ANN models utilize separate 4-factor clastogen- and 4-factor aneugen-detection algorithms, RF uses a single 7-factor clastogen plus aneugen detection algorithm. This endows the LR and ANN models with an ability to generate high clastogen and high aneugen probability scores for the same chemical over the same concentration(s). That is, these biological activities are not mutually exclusive with this approach. Conversely, the single 7-factor RF model places clastogenicity and aneugenicity classifications in a state of competition. Since the biomarker responses for tribromoacetaldehyde were observed to occur over similar concentrations, the net effect was that both sets of probability scores were capped. It is therefore not surprising that RF failed to predict tribromoacetaldehyde as genotoxic while the other models did, and it reinforces the use of ensembles to overcome limitations of any 1 machine learning approach.

CONCLUSIONS

In summary, the *in vitro* MultiFlow DNA Damage assay was found to perform well on a set of chemicals that had not been tested previously in this system. Furthermore, analytic approaches based on supervised machine learning with labeled training set data provided rapid and efficient companion tools for synthesizing multiplexed biomarker data into genotoxicity predictions that exhibit high accuracy, sensitivity, and specificity. In this exercise, the ANN model was a particularly high performing learner, although as has been demonstrated in other fields, ensemble modeling approaches may enhance these predictions (Elder, 2003).

Forty-nine NTP chemicals were not adequately tested (maximum concentration well below the assay's cytotoxicity limit) and/or had insufficient genotoxicity data from conventional assays to allow their genotoxic potential to be defined. For these chemicals, MultiFlow data may represent a good starting point for designing additional studies aimed at more thoroughly characterizing their genotoxic potential.

The flexibility of the MultiFlow assay as described, and the degree to which it has been miniaturized and automated to date, suggest several, nonmutually exclusive placements for the assay, as well as for other assays with similar characteristics. First, they provide a means to collect data on a large number of chemicals in a robotic-sampling compatible, efficient manner. This is relevant for midthroughput testing environments that desire genotoxicity information for new chemicals in early development, and for groups seeking to address the backlog of commercial chemicals with scant genotoxicity profiles. Second, conducting *in vitro* cell-based assays, such as the *in vitro* micronucleus assay, for regulatory requirements and capturing MultiFlow data in parallel may be an efficient means for identifying MoA in the case of a positive finding. In other instances, this parallel testing approach may help provide evidence that the positive *in vitro* finding is not likely to occur *in vivo* (ie, "irrelevant positive"). Third, used in follow-up to a positive finding, MoA information from a multiplexed assay such as MultiFlow, in combination with data that addresses margin of exposure, may be useful for de-risking some consensus genotoxicants.

The encouraging findings presented herein suggest that additional work is warranted to further improve this assay platform. Some priorities for additional research include expanding the number and classes of chemicals tested (eg, nucleoside analogs); determining the compatibility of additional cell lines, some with endogenous metabolic capacity (eg, HepaRG); investigating the use of additional biomarkers, treatment schedules, and/or harvest times in an effort to generate additional MoA insights, eg, elucidation of molecular targets; and further miniaturization of the assay. In addition, it will be of interest to explore the use of other machine learning approaches—ensemble or otherwise—that are able to seamlessly generate genotoxic activity and MoA predictions from MultiFlow-derived biomarkers in concert with other data streams, whether they are accomplished by flow cytometry, or generated by completely different analysis platforms (eg, image analysis or

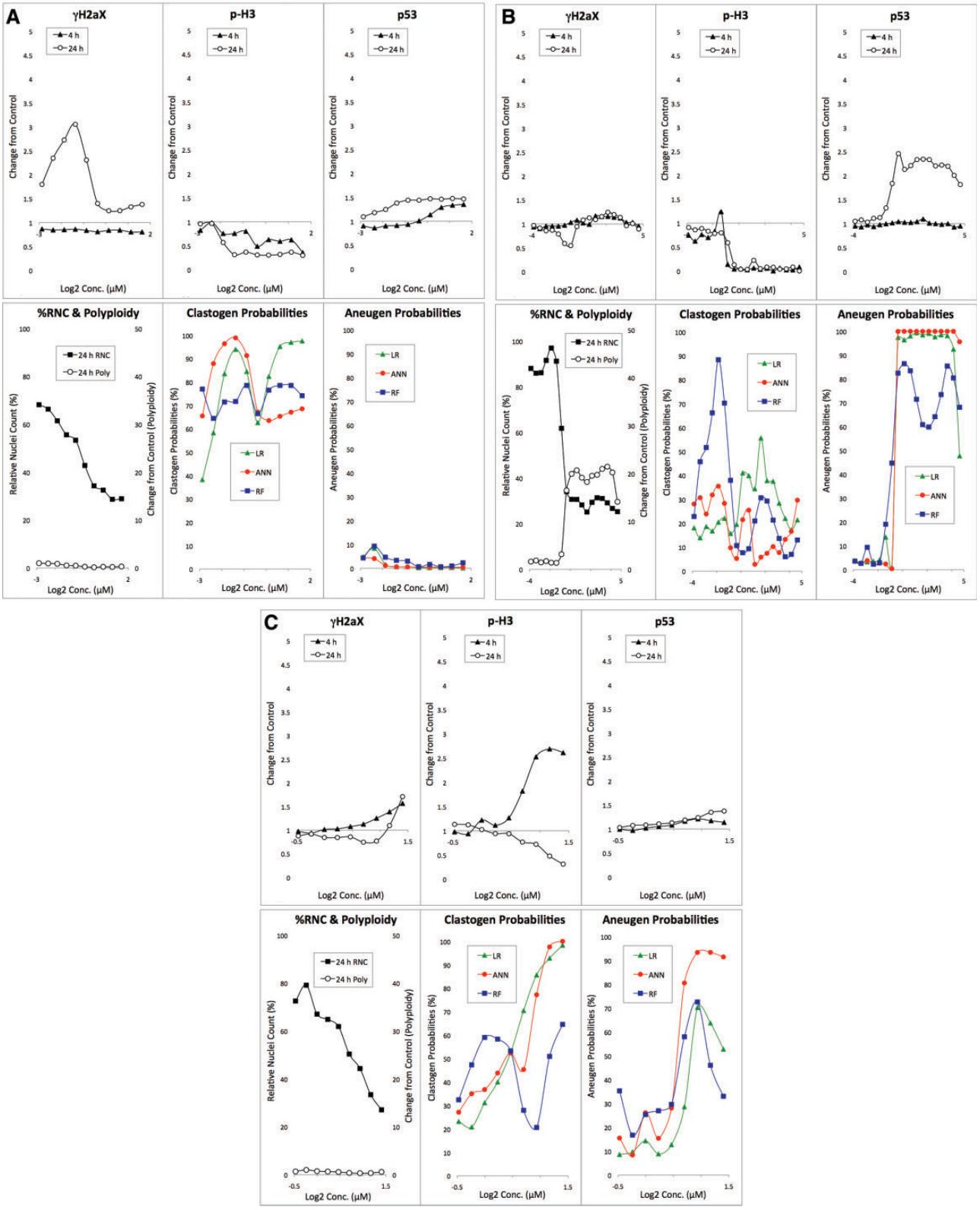

Figure 5. A, Biomarker response data are graphed for 6-thioguanine-exposed TK6 cells versus concentration. The bottom middle panel shows clastogen probabilities as a function of 6-thioguanine concentration based on 3 machine learning algorithms: LR, ANN, and RF. The bottom right panel shows analogous aneugen probability scores. B, Biomarker response data are graphed for ZM-447439-exposed TK6 cells versus concentration. The bottom middle panel shows clastogen probabilities as a function of ZM-447439 concentration based on 3 machine learning algorithms: LR, ANN, and RF. The bottom right panel shows analogous aneugen probability scores. C, Biomarker response data are graphed for tribromoacetaldehyde-exposed TK6 cells versus concentration. The bottom middle panel shows clastogen probabilities as a function of tribromoacetaldehyde concentration based on 3 machine learning algorithms: LR, ANN, and RF. The bottom right panel shows analogous aneugen probability scores.

toxicogenomics). The desirability of effectively synthesizing results from multiple data streams has been a theme articulated by Rusyn and Daston (2010) and more recently by Dertinger (2017), among others.

SUPPLEMENTARY DATA

Supplementary data are available at *Toxicological Sciences* online.

ACKNOWLEDGMENTS

The authors would like to thank Mr Brad Collins, NTP, for his expert assistance in preparing the NTP chemicals and Dr Scott Auerbach, NTP, for careful review of the manuscript and valuable suggestions. Ms Svetlana Avlasevich provided help with benchtop work for which we are grateful. The authors would like to thank the HESI-Genetic Toxicology Testing Committee, particularly the MoA Workgroup, for valuable intellectual contributions. Several colleagues provided excellent recommendations regarding chemicals for testing, and in other cases shared information and expert opinions about conventional genotoxicity assay results. We are indebted to Mr Richard Spellman, Ms Maria Engel, and Dr Maik Schuler, Dr Zhanna Sobol, Dr Ann Doherty, and Dr Elisabeth Lorge for these contributions. S.M.B., D.T.B., J.C.B., and S.D.D. are employed by Litron Laboratories. Litron has a patent covering the flow cytometry-based assay described in this manuscript and sells a commercial kit based on these procedures: MultiFlow DNA Damage Kit—p53, γH2AX, Phospho-Histone H3.

FUNDING

This work was funded by a grant from the National Institute of Health/National Institute of Environmental Health Sciences (NIEHS; grant no. R44ES024039). The contents are solely the responsibility of the authors, and do not necessarily represent the official views of the NIEHS.

REFERENCES

Au, W., and Hsu, T. C. (1979). Studies on clastogenic effects of biologic stains and dyes. *Environ. Mol. Mutagen.* **1**, 27–35.

Audebert, M., Riu, A., Jacques, C., Hillenweck, A., Jamin, E. L., Zalko, D., and Cravedi, J. P. (2010). Use of the γH2AX assay for assessing the genotoxicity of polycyclic aromatic hydrocarbons in human cell lines. *Toxicol. Lett.* **199**, 182–192.

Avlasevich, S. L., Bryce, S. M., Cairns, S. E., and Dertinger, S. D. (2006). In vitro micronucleus scoring by flow cytometry: Differential staining of micronuclei versus apoptotic and necrotic chromatin enhances assay reliability. *Environ. Mol. Mutagen.* **47**, 56–66.

Baldini, E., Tuccilli, C., Prinzi, N., Sorrenti, S., Antonelli, A., Gnessi, L., Catania, A., Moretti, C., Mocini, R., Carbotta, G., *et al.* (2013). The dual aurora kinase inhibitor ZM447439 prevents anaplastic thyroid cancer cell growth and tumorigenicity. *J. Biol. Regul. Homeost. Agents* **27**, 705–715.

Basso, E., Fiore, M., Leone, S., Degrassi, F., and Cozzi, R. (2013). Effects of resveratrol on topoisomerase II-α activity: Induction of micronuclei and inhibition of chromosome segregation in CHO-K1 cells. *Mutagenesis* **28**, 243–248.

Bernacki, D. T., Bryce, S. M., Bemis, J. C., Kirkland, D., and Dertinger, S. D. (2016). γH2AX and p53 responses in TK6 cells discriminate promutagens and nongenotoxicants in the presence of rat liver S9. *Environ. Mol. Mutagen.* **57**, 546–558.

BG RCI Toxicological Evaluations, No. 266. Available at: https://www.bgrci.de/fachwissen-portal/topic-list/hazardous-substances/toxikologische-datensaetze-en/toxikologische-details/r/2-methoxy-23-dihydropyran-3. Accessed August 1, 2017.

Blazak, W. F., Meier, J. R., Stewart, B. E., Blachman, D. C., and Deahl, J. T. (1988). Activity of 1, 1, 1- and 1, 1, 3-trichloroacetones in a chromosomal aberration assay in CHO cells and the micronucleus and spermhead abnormality assays in mice. *Mutat. Res.* **206**, 431–438.

Bryce, S. M., Bemis, J. C., Mereness, J. A., Spellman, R. A., Moss, J., Dickinson, D., Schuler, M. J., and Dertinger, S. D. (2014). Interpreting in vitro micronucleus positive results: Simple biomarker matrix discriminates clastogens, aneugens, and misleading positive agents. *Environ. Mol. Mutagen.* **55**, 542–555.

Bryce, S. M., Bernacki, D. T., Bemis, J. C., and Dertinger, S. D. (2016). Genotoxic mode of action predictions from a multiplexed flow cytometric assay and a machine learning approach. *Environ. Mol. Mutagen.* **57**, 171–189.

Bryce, S. M., Bernacki, D. T., Bemis, J. C., Spellman, R. A., Engel, M. E., Schuler, M., Lorge, E., Heikkinen, P. T., Hemmann, U., Thybaud, V., *et al.* (2017). Interlaboratory evaluation of a multiplexed high information content in vitro genotoxicity assay. *Environ. Mol. Mutagen.* **58**, 146–161.

Camptosar® (Irinotecan) [package insert] Pfizer Inc, NY, NY. (2014). Available at: https://www.accessdata.fda.gov/drugsatfda_docs/label/2014/020571s048lbl.pdf. Accessed August 2, 2017.

Cemeli, E., Carder, J., Anderson, D., Guillamet, E., Morillas, M. J., Creus, A., and Marcos, R. (2003). Antigenotoxic properties of selenium compounds on potassium dichromate and hydrogen peroxide. *Teratogen. Carcinog. Mutagen.* **23**, 53–67.

Cheung, J. R., Dickinson, D. A., Moss, J., Schuler, M. J., Spellman, R. A., and Heard, P. L. (2015). Histone markers identify the mode of action for compounds positive in the TK6 micronucleus assay. *Mutat. Res.* **777**, 7–16.

Cimino, M. C. (2006). Comparative overview of current international strategies and guidelines for genetic toxicology testing for regulatory purposes. *Environ. Mol. Mutagen.* **47**, 362–390.

Dearfield, K. L., Auletta, A. E., Cimino, M. C., and Moore, M. M. (1991). Considerations in the U.S. Environmental Protection Agency's testing approach for mutagenicity. *Mutat. Res.* **258**, 259–283.

Degrassi, F., De Salvia, R., and Berghella, L. (1993). The production of chromosomal alterations by β-lapachone, an activator of topoisomerase I. *Mutat. Res.* **288**, 263–267.

Dertinger, S. D. (2017). Three lessons for genetic toxicology from baseball analytics. *Environ Mol Mutagen* **58**, 390–397.

Diaz, D., Scott, A., Carmichael, P., Shi, W., and Costales, C. (2007). Evaluation of an automated in vitro micronucleus assay in CHO-K1 cells. *Mutat. Res.* **630**, 1–13.

Doherty, A. T., Ellard, S., Parry, E. M., and Parry, J. M. (1996). A study of the aneugenic activity of trichlorfon detected by centromere-specific probes in human lymphoblastoid cell lines. *Mutat. Res.* **372**, 221–231.

EFSA. (2014). Scientific opinion on the safety and efficacy of tannic acid when used as feed flavouring for all animal species. *EFSA J.* **12**, 3828.

Elder, J. (2003). The generalization paradox of ensembles. *J. Comput. Graph. Stat.* **12**, 853–864.

Elliott, A., and Reiners, J. J. Jr. (2008). Suppression of autophagy enhances the cytotoxicity of the DNA-damaging aromatic amine p-anilinoaniline. *Toxicol. Appl. Pharmacol.* **232**, 169–179.

EPA. (2006). Toxicological review of dichlorobenzenes. Available at: https://www.epa.gov/iris. Accessed August 2, 2017.

EURL ECVAM Genotoxicity & Carcinogenicity Consolidated Database of Ames Positive Chemicals. Available at: https://eurl-ecvam.jrc.ec.europa.eu/databases/genotoxicity-carcinogenicity-db. Accessed August 1, 2017.

Fowler, P., Smith, K., Young, J., Jeffrey, L., Kirkland, D., Pfuhler, S., and Carmichael, P. (2012). Reduction of misleading ("false") positive results in mammalian cell genotoxicity assays. I. Choice of cell type. *Mutat. Res.* **742**, 11–25.

Fox, J. T., Sakamuru, S., Huang, R., Teneva, N., Simmons, S. O., Xia, M., Tice, R. R., Austin, C. P., and Myung, K. (2012). High-throughput genotoxicity assay identifies antioxidants as inducers of DNA damage response and cell death. *Proc. Natl. Acad. Sci. U.S.A.* **109**, 5423–5428.

Galloway, S. M. (2017). International regulatory requirements for genotoxicity testing for pharmaceuticals used in human medicine, and their impurities and metabolites. *Environ. Mol. Mutagen.* **58**, 296–324.

Garcia-Canton, C., Anadon, A., and Meredith, C. (2013). Assessment of the in vitro γH2AX assay by high content screening as a novel genotoxicity test. *Mutat. Res.* **757**, 158–166.

Ge, J., Chow, D. N., Fessler, J. L., Weingeist, D. M., Wood, D. K., and Engelward, B. P. (2015). Micropatterned comet assay enables high throughput and sensitive DNA damage quantification. *Mutagenesis* **30**, 11–19.

Gollapudi, P., Hasegawa, L. S., and Eastmond, D. A. (2014). A comparative study of the aneugenic and polyploidy-inducing effects of fisetin and two model Aurora kinase inhibitors. *Mutat. Res.* **767**, 37–43.

Hauf, S., Cole, R. W., LaTerra, S., Zimmer, C., Schnapp, G., Walter, R., Heckel, A., van Meel, J., Rieder, C. L., and Peters, J. M. (2003). The small molecule Hesperadin reveals a role for Aurora B in correcting kinetochore-microtubule attachment and in maintaining the spindle assembly checkpoint. *J. Cell. Biol.* **161**, 281–294.

Hendriks, G., Atallah, M., Morolli, B., Calléja, F., Ras-Verloop, N., Huijskens, I., Raamsman, M., van de Water, B., and Vrieling, H. (2012). The ToxTracker assay: Novel GFP reporter systems that provide mechanistic insight into the genotoxic properties of chemicals. *Toxicol. Sci.* **125**, 285–298.

IARC monograph. (1982). Some aromatic amines, anthraquinones and nitroso compounds, and inorganic fluorides used in drinking-water and dental procedures. Vol 27. Available at: http://monographs.iarc.fr/ENG/Monographs/Vol1-42/mono27.pdf. Accessed August 1, 2017.

Ibrance® (Palbociclib) [package insert] Pfizer Inc, NY, NY. (2015). Available at: https://www.accessdata.fda.gov/drugsatfda_docs/label/2015/207103s000lbl.pdf. Accessed August 2, 2017.

Invirase® (Saquinavir mesylate) [package insert] Roche Laboratories Inc, Nutley, NJ. (2014). Available at: https://www.accessdata.fda.gov/drugsatfda_docs/label/2010/020628s032, 021785s009lbl.pdf. Accessed August 2, 2017.

Irressa® (Gefitinib) [package insert] AstraZeneca Pharmaceuticals LP, Wilmington, DE. (2003). Available at: https://www.accessdata.fda.gov/drugsatfda_docs/label/2003/021399lbl.pdf. Accessed August 2, 2017.

Jeong, C. H., Postigo, C., Richardson, S. D., Simmons, J. E., Kimura, S. Y., Mariñas, B. J., Barcelo, D., Liang, P., Wagner, E. D., and Plewa, M. J. (2015). Occurrence and comparative toxicity of haloacetaldehyde disinfection byproducts in drinking water. *Environ. Sci. Technol.* **49**, 13749–13759.

Kasper, P. (2001). Cyproterone acetate: A genotoxic carcinogen? *Pharmacol. Toxicol.* **88**, 223–231.

Khamphio, M., Barusrux, S., and Weerapreeyakul, N. (2016). Sesamol induces mitochondrial apoptosis pathway in HCT116 human colon cancer cells via pro-oxidant effect. *Life Sci.* **158**, 46–56.

Khoury, L., Zalko, D., and Audebert, M. (2016). Complementarity of phosphorylated histones H2AX and H3 quantification in different cell lines for genotoxicity screening. *Arch. Toxicol.* **90**, 1983–1995.

Kirkland, D., Aardema, M., Henderson, L., and Müller, L. (2005). Evaluation of the ability of a battery of three in vitro genotoxicity tests to discriminate rodent carcinogens and non-carcinogens I. Sensitivity, specificity and relative predictivity. *Mutat. Res.* **584**, 1–256.

Kirkland, D., Kasper, P., Martus, H. J., Müller, L., van Benthem, J., Madia, F., and Corvi, R. (2016). Updated recommended lists of genotoxic and non-genotoxic chemicals for assessment of the performance of new or improved genotoxicity tests. *Mutat. Res.* **795**, 7–30.

Klimberg, R., and McCullough, B. D. (2016) *Fundamentals of Predictive Analytics with JMP®*. 2nd ed. SAS Institute Inc., Cary, NC, USA.

Kurihara, D., Matsunaga, S., Kawabe, A., Fujimoto, S., Noda, M., Uchiyama, S., and Fukui, K. (2006). Aurora kinase is required for chromosome segregation in tobacco BY-2 cells. *Plant J.* **48**, 572–580.

Le Curieux, F., Marzin, D., and Erb, F. (1994). Study of the genotoxic activity of five chlorinated propanones using the SOS chromotest, the Ames-fluctuation test and the newt micronucleus test. *Mutat. Res.* **341**, 1–15.

Lefevre, P. A., and Ashby, J. (1981). The effects of pre-incubation period and norharman on the mutagenic potency of 4-dimethylaminoazobenzene and 3'-methyl-4-dimethylaminoazobenzene in S. typhimurium. *Carcinogenesis* **2**, 927–931.

Leone, S., Basso, E., Polticelli, F., and Cozzi, R. (2012). Resveratrol acts as a topoisomerase II poison in human glioma cells. *Int. J. Cancer* **131**, E173–E178.

Li, H. H., Hyduke, D. R., Chen, R., Heard, P., Yauk, C. L., Aubrecht, J., and Fornace, A. J. Jr. (2015). Development of a toxicogenomics signature for genotoxicity using a dose-optimization and informatics strategy in human cells. *Environ. Mol. Mutagen.* **56**, 505–519.

Liviac, D., Creus, A., and Marcos, R. (2009). Genotoxicity analysis of two hydroxyfuranones, byproducts of water disinfection, in human cells treated in vitro. *Environ. Mol. Mutagen.* **50**, 413–420.

Lynch, A. M., and Parry, J. M. (1993). The cytochalasin-B micronucleus/kinetochore assay in vitro: Studies with 10 suspected aneugens. *Mutat. Res.* **287**, 71–86.

MacGregor, J. T., Wehr, C. M., Henika, P. R., and Shelby, M. D. (1990). The in vivo erythrocyte micronucleus test: Measurement at steady state increases assay efficiency and permits integration with toxicity studies. *Fundam. Appl. Toxicol.* **14**, 513–522.

Matsuoka, A., Isama, K., and Tsuchiya, T. (2005). In vitro induction of polyploidy and chromatid exchanges by culture medium extracts of natural rubbers compounded with 2-mercaptobenzothiazole as a positive control candidate for genotoxicity tests. *J. Biomed. Mater. Res. A* **75A**, 439–444.

Mercado-Feliciano, M., Cora, M. C., Witt, K. L., Granville, C. A., Hejtmancik, M. R., Fomby, L., Knostman, K. A., Ryan, M. J.,

Newbold, R., Smith, C., *et al*. (2012). An ethanolic extract of black cohosh causes hematological changes but not estrogenic effects in female rodents. *Toxicol. Appl. Pharmacol*. **263**, 138–147.

Mittelstaedt, R. A., Mei, N., Webb, P. J., Shaddock, J. G., Dobrovolsky, V. N., McGarrity, L. J., Morris, S. M., Chen, T., Beland, F. A., Greenlees, K. J., *et al*. (2004). Genotoxicity of malachite green and leucomalachite green in female Big Blue B6C3F1 mice. *Mutat. Res*. **561**, 127–138.

Muehlbauer, P. A., and Schuler, M. J. (2005). Detection of numerical chromosome aberrations by flow cytometry: A novel process for identifying aneugenic agents. *Mutat. Res*. **585**, 156–169.

Muehlbauer, P. A., Spellman, R. A., Gunther, W. C., Sanok, K. E., Wiersch, C. J., O'Lone, S. D., Dobo, K. L., and Schuler, M. J. (2008). Improving dose selection and identification of aneugens in the in vitro chromosome aberration test by integration of flow cytometry-based methods. *Environ. Mol. Mutagen*. **49**, 318–327.

Müller, L., Kasper, P., and Kaufmann, G. (1992). The clastogenic potential in vitro of pyrrolizidine alkaloids employing hepatocyte metabolism. *Mutat. Res. Lett*. **282**, 169–176.

Nakamuro, K., Yoshikawa, K., Sayato, Y., Kurata, H., Tonomura, M., and Tonomura, A. (1976). Studies on selenium-related compounds. V. Cytogenetic effect and reactivity with DNA. *Mutat. Res*. **40**, 177–183.

NTP Technical Report on the Toxicology Studies of Malachite Green Chloride and Leucomalachite Green. (2004). Toxicity Report Series Number 71. Available at https://ntp.niehs.nih.gov/ntp/htdocs/st_rpts/tox071.pdf. Accessed August 1, 2017.

Nagel, Z. D., Margulies, C. M., Chaim, I. A., McRee, S. K., Mazzucato, P., Ahmad, A., Abo, R. P., Butty, V. L., Forget, A. L., and Samson, L. D. (2014). Multiplexed DNA repair assays for multiple lesions and multiple doses via transcription inhibition and transcriptional mutagenesis. *Proc. Natl. Acad. Sci. U.S.A*. **111**, E1823–E1832.

Nikolova, T., Dvorak, M., Jung, F., Adam, I., Krämer, E., Gerhold-Ay, A., and Kaina, B. (2014). γH2AX assay for genotoxic and nongenotoxic agents: Comparison of H2AX phosphorylation with cell death response. *Toxicol. Sci*. **140**, 103–117.

Nishihara, K., Huang, R., Zhao, J., Shahane, S. A., Witt, K. L., Smith-Roe, S. L., Tice, R. R., Takeda, S., and Xia, M. (2016). Identification of genotoxic compounds using isogenic DNA repair deficient DT40 cell lines on a quantitative high throughput screening platform. *Mutagenesis* **31**, 69–81.

Ohshima, H., Friesen, M., Malaveille, C., Brouet, I., Hautefeuille, A., and Bartsch, H. (1989). Formation of direct-acting genotoxic substances in nitrosated smoked fish and meat products: Identification of simple phenolic precursors and phenyldiazonium ions as reactive products. *Food Chem. Toxicol*. **27**, 193–203.

Ray, J. H., and Altenburg, L. C. (1980). Dependence of the sister-chromatid exchange-inducing abilities of inorganic selenium compounds on the valence state of selenium. *Mutat. Res*. **78**, 261–266.

REACH Monitor. (2012). Anthraquinone: Genotoxicity and carcinongenicity potential of different manufacturing origins. Available at: https://echa.europa.eu/documents/10162/13579/clh_doc_1_en.pdf. Accessed August 2, 2017.

Rusyn, I., and Daston, G. P. (2010). Computational toxicology: Realizing the promise of the toxicity testing in the 21st century. *Environ. Health Perspect*. **118**, 1047–1050.

Savia, L. A., Leal, P. C., Vieira, T. O., Rosso, R., Nunes, R. J., Yunes, R. A., Creczynski-Pasa, T. B., Barardi, C. R. M., and Simoes, C. M. O. (2005). Evaluation of anti-herpetic and antioxidant activities, and cytotoxic and genotoxic effects of synthetic alkyl-esters of gallic acid. *Arzneim-Forsch/Drug Res*. **55**, 66–75.

Shahin, M. M. (1989). Evaluation of the mutagenicity of azo dyes in *Salmonella typhimurium*: A study of structure-activity relationships. *Mutagenesis* **4**, 115–125.

Sideris, E. G., Charalambous, S. C., Tsolomyty, A., and Katsaros, N. (1988). Mutagenesis; carcinogenesis and the metal elements—DNA interaction. *Prog. Clin. Biol. Res*. **259**, 13–25.

Smart, D. J., Ahmedi, K. P., Harvey, J. S., and Lynch, A. M. (2011). Genotoxicity screening via the γH2AX by flow assay. *Mutat. Res*. **715**, 25–31.

Søderlund, E. J., Nelson, S. D., and Dybing, E. (1979). Mutagenic activation of tri(2, 3-dibromopropyl)phosphate: The role of microsomal oxidative metabolism. *Acta Pharmacol. Toxicol*. **45**, 112–121.

Sprycel® (dasatinib) [package insert] Bristol-Myers Squibb Co, Princeton, NJ. (2010). Available at: https://www.accessdata.fda.gov/drugsatfda_docs/label/2010/021986s7s8lbl.pdf. Accessed August 2, 2017.

Stich, H. F., Rosin, M. P., Wu, C. H., and Powrie, W. D. (1981). The action of transition metals on the genotoxicity of simple phenols, phenolic acids and cinnamic acids. *Cancer Lett*. **14**, 251–260.

Stopper, H., Körber, C., Gibis, P., Spencer, D. L., and Caspary, W. J. (1995). Micronuclei induced by modulators of methylation: Analogs of 5-azacytidine. *Carcinogenesis* **16**, 1647–1650.

Tagrisso™ (Osimertinib) [package insert] AstraZeneca Pharmaceuticals LP, Wilmington, DE. (2012). Available at: https://www.accessdata.fda.gov/drugsatfda_docs/label/2015/208065s000lbl.pdf. Accessed August 2, 2017.

Tice, R. R., Austin, C. P., Kavlock, R. J., and Bucher, J. R. (2013). Improving the human hazard characterization of chemicals: A Tox21 update. *Environ. Health Perspect*. **121**, 756–765.

Tinkler, J., Gott, D., and Bootman, J. (1998). Risk assessment of dithiocarbamate accelerator residues in latex-based medical devices: Genotoxicity considerations. *Food Chem. Toxicol*. **36**, 849–866.

Tsutsui, T., Tamura, Y., Yagi, E., Someya, H., Hori, I., Metzler, M., and Barrett, J. C. (2003). Cell-tranforming activity and mutagenicity of 5 phytoestrogens in cultured mammalian cells. *Int. J. Cancer* **105**, 312–320.

Vanni, A., Fiore, M., De Salvia, R., Cundari, E., Ricordy, R., Ceccarelli, R., and Degrassi, F. (1998). DNA damage and cytotoxicity induced by beta-lapachone: Relationship to poly(ADP-ribose) polymerase inhibition. *Mutat. Res*. **401**, 55–63.

Witt, K. L., Hsieh, J. H., Smith-Roe, S. L., Xia, M., Huang, R., Zhao, J., Auerbach, S. S., Hur, J., and Tice, R. R. (2017). Assessment of the DNA damage potential of environmental chemicals using a quantitative high-throughput screening approach to measure p53 activation. *Environ. Mol. Mutagen*. **58**, 494–507.

Wu, P., Nielsen, T. E., and Clausen, M. H. (2015). FDA-approved small-molecule kinase inhibitors. *Trends Pharm. Sci*. **36**, 422–439.

Yamamoto, K. N., Hirota, K., Kono, K., Takeda, S., Sakamuru, S., Xia, M., Huang, R., Austin, C. P., Witt, K. L., and Tice, R. R. (2011). Characterization of environmental chemicals with potential for DNA damage using isogenic DNA repair-deficient chicken DT40 cell lines. *Environ. Mol. Mutagen*. **52**, 547–561.

Yauk, C. L., Buick, J. K., Williams, A., Swartz, C. D., Recio, L., Li, H.-H., Fornace, A. J., Thomson, E. M., and Aubrecht, J. (2016). Application of the TGx-28.65 transcriptomic biomarker to classify genotoxic and non-genotoxic chemicals in human TK6 cells in the presence of rat liver S9. *Environ. Mol. Mutagen*. **57**, 243–260.